

# Cloning, expression and interaction of human T-cell receptors with the bacterial superantigen SSA

Mauricio C. De Marzi<sup>1</sup>, Marisa M. Fernández<sup>1</sup>, Eric J. Sundberg<sup>2</sup>, Luciana Molinero<sup>3</sup>, Norberto W. Zwirner<sup>3</sup>, Andrea S. Llera<sup>1,\*</sup>, Roy A. Mariuzza<sup>2</sup> and Emilio L. Malchiodi<sup>1</sup>

<sup>1</sup>Cátedra de Inmunología and Instituto de Estudios de la Inmunidad Humoral (IDEHU), CONICET, Facultad de Farmacia y Bioquímica, Universidad de Buenos Aires, Argentina; <sup>2</sup>Center for Advanced Research in Biotechnology, W. M. Keck Laboratory for Structural Biology, University of Maryland Biotechnology Institute, Rockville, MD, USA; <sup>3</sup>Laboratorio de Inmunogenética, Hospital de Clínicas José de San Martín, Facultad de Medicina, Universidad de Buenos Aires, Argentina

Superantigens (SAGs) are a class of disease-causing and immunostimulatory proteins of bacterial or viral origin that activate a large number of T-cells through interaction with the V $\beta$  domain of T-cell receptors (TCRs). In this study, recombinant TCR  $\beta$  chains were constructed with human variable domains V $\beta$ 5.2, V $\beta$ 1 and V $\beta$ 2.1, expressed as inclusion bodies, refolded and purified. The *Streptococcus pyogenes* SAG SSA-1 was cloned and expressed as a soluble periplasmic protein. SSA-1 was obtained both as a monomer and a dimer that has an intermolecular disulfide bond. We analyzed the biological activity of the recombinant SAGs by proliferation assays. The results suggest that SSA dimerization occludes the TCR interaction site. Naturally occurring

SSA dimerization was also observed in supernatants of *S. pyogenes* isolates. An SSA mutant [SSA(C26S)] was produced to eliminate the Cys responsible for dimerization. Affinity assays using a resonant biosensor showed that both the mutant and monomeric wild type SSA have affinity for human V $\beta$ 5.2 and V $\beta$ 1 with  $K_d$  of 9–11  $\mu$ M with a fast  $k_{\text{ass}}$  and a moderately fast  $k_{\text{diss}}$ . In spite of the reported stimulation of V $\beta$ 2.1 bearing T-cells by SSA, we observed no measurable interaction.

**Keywords:** affinity constant; biosensor; SSA; *Streptococcus pyogenes*; T-cell receptor.

T-lymphocytes recognize a wide variety of antigens through highly diverse cell-surface glycoproteins known as T-cell receptors (TCRs). These disulfide-linked heterodimers are comprised of  $\alpha$  and  $\beta$  (or  $\gamma$  and  $\delta$ ) chains that have variable (V) and constant (C) regions homologous to those of antibodies. Unlike antibodies, which recognize antigen alone,  $\alpha\beta$  TCRs recognize antigen only in the form of peptides bound to major histocompatibility complex (MHC) molecules. In addition TCRs interact with a class of viral and bacterial proteins known as superantigens (SAGs).

SAGs are microbial toxins with potent immunostimulatory properties. They circumvent the normal mechanism for T-cell activation by binding as unprocessed molecules to

MHC class II and TCR. The resulting trimolecular complex activates a large fraction of the T-cell population (5–20% of all T-cells), compared with conventional peptide antigen specific activation (0.01–0.001%). The activated T-cells release massive amounts of inflammatory cytokines such as IL-2, TNF- $\alpha$  and IFN- $\gamma$ , contributing to the symptoms caused by SAGs, which can lead to lethal toxic shock [1]. SAGs have been implicated in a number of autoimmune diseases such as diabetes mellitus, rheumatoid arthritis and multiple sclerosis, by activating T-cells specific for self-antigens [2,3]; however, the best characterized diseases caused by SAGs are food poisoning and toxic shock syndrome (TSS) [4,5].

SAGs produced by several strains of *Staphylococcus aureus* and *Streptococcus pyogenes* are structurally and immunologically the best characterized to date [6], although the crystal structures of SAGs from *Mycoplasma arthritidis* and *Yersinia pseudotuberculosis* have been solved recently [7,8]. Bacterial SAGs are 22–29 kDa molecules that are resistant to proteases and heat denaturalization. They can be absorbed by epithelial cells as immunologically intact proteins [1,9]. Most SAGs share a common three-dimensional structure, although their amino acid sequences are highly variable. The structure of bacterial SAGs shows two globular domains: a small N-terminal domain with an OB fold ('oligosaccharide/oligonucleotide-binding'), and a large C-terminal domain with a  $\beta$ -grasp motif [10,11]. The TCR binding site on the SAG is situated in a cleft between the two domains [12,13]. In addition, SAGs have one or two binding sites for MHC class II: a low affinity site, and a higher

Correspondence to E. L. Malchiodi, Junín 956 4° P Inmunología (1113) Buenos Aires, Argentina. Fax: +54 11 4964 0024, Tel.: +54 11 4964 8260, E-mail: emalchio@fbyb.uba.ar

**Abbreviations:** C, constant region; DTT, dithiothreitol; MHC, major histocompatibility complex; NTA, nitrilotriacetic acid; PBMC, peripheral blood mononuclear cell; SAG, superantigen; SEC3, Staphylococcal enterotoxin C3; SSA, Streptococcal superantigen; SSAm, SSA monomer; SSAd, SSA dimer; SSAia, SSA-iodoacetamide; TCR, T-cell receptor; TSS, toxic shock syndrome; V, variable region; wt, wild type.

\*Present address: Fundación Instituto Leloir, CONICET, Buenos Aires, Argentina.

(Received 26 May 2004, revised 20 August 2004, accepted 26 August 2004)

affinity site on the opposite face of the molecule that is Zn<sup>2+</sup> dependent [14,15].

The proinflammatory and procytotoxic properties of SAGs are responsible for the increased interest in these molecules in the treatment of several pathologies and because of the potential use of the toxins as biological weapons. Alteration of their MHC and TCR binding capacity by site directed mutagenesis could be useful in the development of vaccines and in cancer therapy. SAGs with mutated TCR and/or MHC binding sites could be employed as vaccines against TSS and food poisoning to generate protective antibodies without systemic effects [16,17].

Streptococcal superantigen (SSA) is a 260 residue protein produced by *S. pyogenes* that can generate symptoms similar to TSS [18]. SSA shares more molecular properties with the staphylococcal enterotoxins SEB and SEC than with other streptococcal SAGs [19]. Cellular proliferation studies show disagreement about which TCR bearing T-cell subsets are expanded by interaction with SSA. Some authors indicated clonal expansion of T-cells bearing human V $\beta$ 3, V $\beta$ 12, V $\beta$ 17 and V $\beta$ 19 [20]. Others showed proliferation of human T-cells bearing V $\beta$ 1, V $\beta$ 2, V $\beta$ 3, V $\beta$ 5.2, V $\beta$ 12, V $\beta$ 15 and V $\beta$ 17 domains and found differences in the stimulation pattern between native and recombinant SSA, or even between variants (SSA-1 or SSA-2) [19,21].

To investigate SSA–TCR binding affinity, we expressed these molecules in high yield prokaryotic systems that allow us to obtain enough recombinant protein to conduct binding studies. In order to avoid dimerization, SSA Cys26 was mutated to Ser [SSA(C26S)]. Different SSA preparations were used to study T-cell proliferation capacity with human peripheral blood mononuclear cells (PBMCs). The binding of SSA and mutant C26S to soluble TCR  $\beta$ -chain molecules V $\beta$ 1, V $\beta$ 2.1 and V $\beta$ 5.2 was measured in real time by a 'resonant mirror' optical biosensor method.

## Materials and methods

### Reagents

All chemicals were of analytical grade and purchased from Sigma (St. Louis, MO). Restriction enzymes, *Taq* DNA polymerase, T4 ligase and buffers for cloning were purchased from New England Biolabs, Inc. (Beverly, MA). Ultra pure agarose was purchased from Gibco BRL-Life Technologies (Rockville, MD).

### Recombinant TCR $\beta$ chains

Human V $\beta$ 5.2 (hV $\beta$ 5.2) was fused to a mouse constant  $\beta$  chain domain (mC $\beta$ 15) to facilitate purification and increase yield [22,23]. Chimeric hV $\beta$ 5.2mC $\beta$ 15 was cloned into the kanamycin resistant expression vector pET26b and expressed as inclusion bodies [12] in *Escherichia coli* BL21(DE3) (Stratagene, La Jolla, CA). Two other  $\beta$  chains, hV $\beta$ 2.1hC $\beta$ 2 and hV $\beta$ 1hC $\beta$ 2 (genes kindly provided by U. Utz and R. P. Sekaly, University of Montreal, Canada), were cloned between the *Nde*I and *Eco*RI restriction sites of the pET17b expression vector and expressed in *E. coli* BL21(DE3) as inclusion bodies. Glycerol stocks of these clones were maintained at  $-70$  °C.

### TCR production and purification

Luria–Bertani broth (LB) agar plates containing 50  $\mu\text{g}\cdot\text{mL}^{-1}$  of kanamycin or 100  $\mu\text{g}\cdot\text{mL}^{-1}$  of ampicillin were incubated overnight at 37 °C from transforming BL21(DE3) glycerol stocks. One litre of LB medium was inoculated with 10 mL overnight culture and grown with shaking at 37 °C to an attenuation of 0.8 at 600 nm. TCR expression was induced with 1 mM isopropyl thio- $\beta$ -D-galactoside for 3–5 h. Cells were harvested by centrifugation at 2100 *g* for 20 min. The bacterial pellet of hV $\beta$ 5.2mC $\beta$ 15 was resuspended in lysis buffer [50 mM Tris/HCl, pH 7.5, 1 mM EDTA, pH 8, and 1 mM dithiothreitol (DTT)] and passed through a French press twice at 1300 psi. The lysate was centrifuged at 7700 *g* for 15 min and the pelleted inclusion bodies were washed four times with 0.5% (v/v) Triton X-100 and 100 mM NaCl in lysis buffer. The inclusion bodies were then washed with 2 M urea in 2 M NaCl, 50 mM Tris/HCl, pH 7.5, 1 mM DTT, with 4 M urea in the same buffer, and finally with 100 mM Tris/HCl, pH 7.5, 1 mM EDTA and 1 mM DTT. Inclusion bodies were then solubilized in 8 M urea, 100 mM Tris/HCl, pH 7.5, 10 mM EDTA and 1 mM DTT. Concentration of solubilized inclusion bodies was estimated in a Coomassie Blue stained SDS/PAGE, using different concentrations of BSA and then diluted 1 : 5 in 6 M guanidine, 10 mM acetate buffer, pH 4.2, and 10 mM EDTA. Denatured  $\beta$  chain was added dropwise to the renaturation buffer (1 M arginine/HCl, pH 7.5, 2 mM EDTA, 100 mM Tris/HCl, pH 7.5, 6.3 mM cysteamine, 3.7 mM cystamine) under vigorous stirring to a final concentration of 20–50  $\mu\text{g}\cdot\text{mL}^{-1}$  during 48 h at 4 °C.

Refolded hV $\beta$ 5.2mC $\beta$ 15 was concentrated and dialyzed extensively against NaCl/P<sub>i</sub> and affinity purified using the anti-mouse C $\beta$  mAb (H57-597) [24,25]. Alternatively, hV $\beta$ 5.2mC $\beta$ 15 was run on a Superdex 200 FPLC column (Amersham Pharmacia Biotech AB, Uppsala, Sweden) to eliminate aggregated material that could interfere with affinity measurements [26]. hV $\beta$ 5.2mC $\beta$ 15 was dialyzed against 50 mM Mes, pH 6, and further purified on a Mono-S cation-exchange FPLC column (Amersham Pharmacia Biotech AB) equilibrated with 50 mM MES, pH 6, and developed with a linear NaCl gradient. The purified protein was dialyzed against NaCl/P<sub>i</sub> and concentrated to 2  $\text{mg}\cdot\text{mL}^{-1}$ .

hV $\beta$ 2.1hC $\beta$ 2 and hV $\beta$ 1hC $\beta$ 2 were also produced as inclusion bodies and refolded at pH 8.5. Purification steps included gel filtration on a Superdex 200 FPLC column and further purification on a Mono Q anion-exchange FPLC column (Amersham Pharmacia Biotech AB) equilibrated with 50 mM Tris, pH 8.5, and developed with a linear NaCl gradient.

### *Streptococcus pyogenes* superantigen (SSA)

The *ssa-1* gene was PCR amplified from *Streptococcus pyogenes* DNA (ATCC 51500 strain) or clinical isolates of *S. pyogenes* with 5' and 3' terminal oligonucleotides specific for the region encoding the mature protein (5' primer, 5'-CATGCCATGGCCAGTAGTCAGCCTGACCCTACTCCAG-3'; 3' primer, 5'-CGCGCGGGATCCTTAGTGATGGTGATGGTGATGGGTGACCGGTTTTTTGG



[<sup>3</sup>H]thymidine was added for the next 18 h and then harvested onto glass fibre filters. Incorporation of radioactivity was then measured using a Liquid Scintillation Analyzer 1600 TR (Packard, Canberra, Australia). All measurements were made in triplicate.

### Binding analysis

The interaction of soluble  $\beta$  chains with SAGs was monitored in a resonance mirror with an IAsys instrument (Labsystem, Cambridge, UK) biosensor, which allows determination of real time interactions between two molecules [28].

$\beta$  Chains or SAGs ( $\approx 100 \mu\text{g}\cdot\text{mL}^{-1}$ ) were dialyzed against 10 mM sodium acetate, pH 5.5, and coupled to the carboxymethyl-dextran cuvettes (Labsystems) using the Amine Coupling Kit as described by the manufacturer [29]. The activation and immobilization periods were set between 5 and 7 min to couple the desired amount of proteins yielding between 400 and 600 arc seconds.

Micromolar concentrations of SAGs [SSA and SSA(C26S)] or  $\beta$  chains (V $\beta$ 1, V $\beta$ 2.1 and V $\beta$ 5.2) were dialyzed against NaCl/P<sub>i</sub>, pH 7.5, containing 0.05% (v/v) Tween 20. Twofold dilutions were made in the same buffer (160, 80, 40, 20, 10, 5, 2.5 and 1.25  $\mu\text{M}$ ). All binding experiments were performed at 25 °C. Dissociation was carried out in (NaCl/P<sub>i</sub>)/Tween 20. Pulses of 10 mM HCl were used to regenerate the surface. All the experiments were repeated at least three times.

Dissociation constants ( $K_d$ ) were determined under equilibrium binding conditions using Scatchard plots after correction for nonspecific binding, in which the proteins were passed over blocked, empty cuvettes, as described previously [26,30]. The off rate ( $k_{\text{diss}}$ ) was determined using the software FASTPLOT and the on rate ( $k_{\text{ass}}$ ) was obtained as  $k_{\text{ass}} = k_{\text{diss}}/K_d$ .

## Results

### TCR $\beta$ chains

Our TCR  $\beta$  chain expression systems yielded 35–50  $\text{mg}\cdot\text{L}^{-1}$  of inclusion bodies. After refolding and concentration, a first purification step was carried out for chimeric hV $\beta$ 5.2mC $\beta$ 15 with a H57-597 mAb affinity column or with an S-200 column, followed by ion exchange chromatography. Typically, a final yield of 1–2  $\text{mg}\cdot\text{L}^{-1}$  of culture for the refolded  $\beta$  chain TCR constructs were obtained.

### Superantigen

Our expression system produced 15  $\text{mg}\cdot\text{L}^{-1}$  of folded wild type SSA-1. After Ni-NTA purification, two bands of protein were observed in SDS/PAGE (Fig. 1A). The weaker band has an apparent molecular mass in agreement with the theoretical value calculated from the amino acid sequence; the stronger band has about twice the expected molecular mass. Both bands were reactive in immunoblotting with anti-His mAbs and an anti-SSA serum prepared in rabbits (Fig. 1C), indicating the presence of two recombinant species. The dimer/monomer mixture could not be efficiently resolved using an

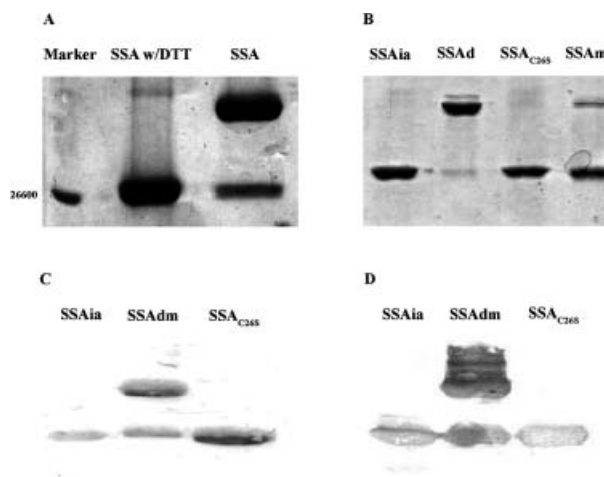


**Fig. 1.** SDS/PAGE and immunoblotting analysis of SSA. (A) 12.5% SDS/PAGE of SSA after Ni-NTA purification (Lane 3) and the same sample treated with DTT (Lane 2). A TCR  $\beta$  chain with a similar molecular mass is shown as a marker (Lane 1). (B) 12.5% SDS/PAGE of different SSA preparations. Lane 1: SSA reduced and alkylated with iodoacetamide (SSAia); Lane 2: SSA preparation enriched in dimer after purification on S75 FPLC (SSAd); Lane 3: C26S mutant (SSA<sub>C26S</sub>) and Lane 4: SSA preparation enriched in monomer (SSAm). (C and D) Immunoblots of SSAia, wtSSA and SSA(C26S) using a commercial anti-His mAb or rabbit anti-SSA sera, respectively.

S75 column, yielding a fraction with 80% monomer (SSAm) and another containing 90% dimer (SSAd) (Fig. 1B). To determine whether an intermolecular disulfide bond mediated dimerization, Ni-NTA purified SSA was gently treated with DTT and the resulting free Cys residues were alkylated with iodoacetamide. As shown in Fig. 1B, reduction and alkylation produced only one band in SDS/PAGE with the expected molecular mass of the monomer.

Considering that dimerization could occlude the TCR binding site, we also constructed a mutant SSA by site-directed mutagenesis. Analysis of the three-dimensional structure of SSA [31] showed that: (a) SSA has five Cys, of which two (Cys93 and Cys108) form a disulfide bond, which is present in most of the known SAGs; (b) the position of Cys101 was not determined in the crystal structure of SSA because it forms part of a loop that could not be modeled; and (c) Cys158 would not be exposed at the SSA surface. The putative TCR binding site of SSA is not known yet but an analysis based on homology with the TCR binding site of SEB and SEC3 [12,13,19,21], showed that Cys26 is not only exposed in the protein surface (Fig. 2), but would be in the putative TCR binding site. Consequently, a point mutation was introduced to replace Cys26 by Ser, which was confirmed by DNA sequencing. As can be seen in Fig. 1B–D, expression of the mutant yields only monomeric SSA, free of dimer.

### T-cell proliferation assay

We next analyzed the ability of recombinant SSA to stimulate human T-cells. All SSA preparations yielded

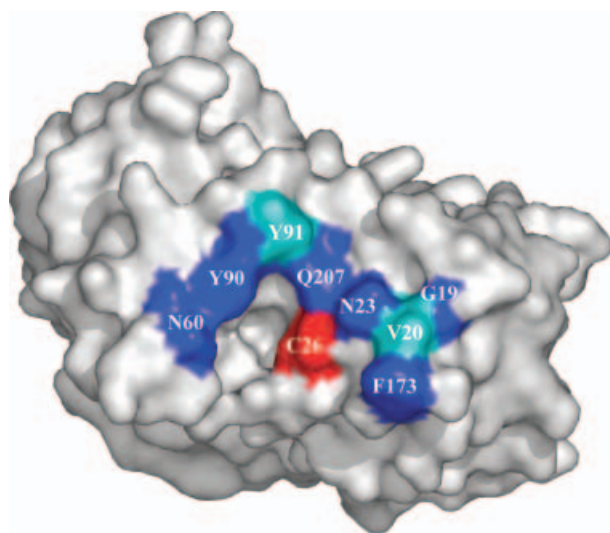


**Fig. 2. SSA three-dimensional structure.** Residue Cys26 of SSA is contiguous with its putative binding interface with the T-cell receptor. The common residues of SEB and SEC3 that form their respective molecular interfaces with mV $\beta$ 8.2 are largely conserved in SSA. These include residues that are strictly conserved between SEB, SEC3 and SSA (shown in blue on the SSA molecular surface), as well as residues that vary between the three superantigens (shown in cyan). Residue Cys26 is shown in red.

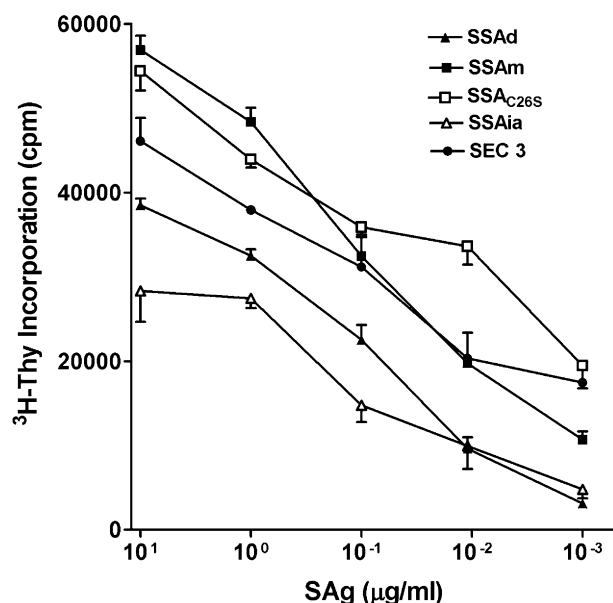


**Fig. 3. Dose-dependent T-cell proliferation by the different SAg preparations.** As indicated in Materials and methods, [<sup>3</sup>H]thymidine incorporation was measured in a liquid scintillation analyzer. Both SSAm and SSA(C26S) produce more than 100-fold higher T-cell proliferation than SSAd and SSAia. SEC3 was included as a positive control.

dose-dependent T-cell proliferation, analyzed by [<sup>3</sup>H]thymidine incorporation (Fig. 3). SSAm and the mutant SSA(C26S) caused greater proliferation than the positive control SAg, SEC3. Both SSAd and SSAia

produced T-cell proliferation > 100-fold lower than SSAm or SSA(C26S) (Fig. 3).

### Affinity assays

Equilibrium and kinetic parameters for SSA binding to different TCR  $\beta$  chains were determined in a resonance mirror using an IAsys instrument biosensor. SSA affinity for the immobilized TCR V $\beta$ 5.2 was first measured and data were evaluated by Scatchard plot analysis. Dissociation constants were estimated from the negative reciprocal of the slope of the fitted line yielding a  $K_d$  value of 153  $\mu$ M (result not shown). Considering that the immobilization process could alter the molecule, rendering inaccurate results, and the fact that a high proportion of SSA was a dimer that may have the TCR binding site blocked, the purified SSAm form and the mutant SSA(C26S) were immobilized in a dextran matrix. As shown in Fig. 4, TCR V $\beta$ 5.2 concentration-dependent binding to both SSA species was observed. The association rate constant ( $k_{\text{ass}}$ ) was too fast to be accurately measured. On the contrary, the dissociation rate constant ( $k_{\text{diss}}$ ) could be determined using higher concentrations of SSA. Therefore, affinities ( $K_d$ ) were determined under equilibrium binding conditions, in which we took report points for Scatchard analysis 5 min after injection. The  $k_{\text{ass}}$  were further calculated using equation  $K_d = k_{\text{diss}}/k_{\text{ass}}$  (Table 1). Immobilization of the SAGs instead of TCRs yielded a higher binding constant of the former, which was similar for both complexes, wtSSA-V $\beta$ 5.2 and SSA(C26S)-V $\beta$ 5.2.

Different concentrations of human V $\beta$ 2.1 and V $\beta$ 1 TCRs were also used to measure the binding to the immobilized SSAm and SSA(C26S). V $\beta$ 1 showed a pattern of association and dissociation rates similar to the one obtained with V $\beta$ 5.2 (Fig. 5), yielding  $K_d$ s of the same order of magnitude (Table 1). On the contrary, no binding of V $\beta$ 2.1 TCR to SSA was detected even using a 160  $\mu$ M concentration of  $\beta$  chain. Trials using higher concentrations were unsuccessful due to nonspecific aggregation of the V $\beta$ 2.1 TCR.

### Discussion

The expression and purification of TCRs using either prokaryotic or eukaryotic systems had been troublesome for several years, delaying structural and other studies. The TCR  $\beta$  chain constructions we engineered allowed us to obtain large amounts of recombinant protein as inclusion bodies that could be refolded properly and used for SAg binding experiments.

SAg constructs generated large amounts of properly folded protein, but monomer and dimer forms were obtained in the wtSSA preparation. Dimerization as a prerequisite for T-cell activation has been suggested for other SAGs, such as SED [32], SPEC [33] and more recently SPEA [34]. In SED and SPEA the presence of  $\text{Zn}^{2+}$  plays an important role in dimerization;  $\text{Zn}^{2+}$  was found in the crystal structure of SPEC after soaking the crystal in a zinc solution, but dimerization of this SAg also occurred in absence of  $\text{Zn}^{2+}$ . On the other hand, SSA, which has not been reported to have a zinc-binding site, dimerized through Cys. Among the known SAGs, most have two Cys residues forming an intramolecular bridge. There are four SAGs with

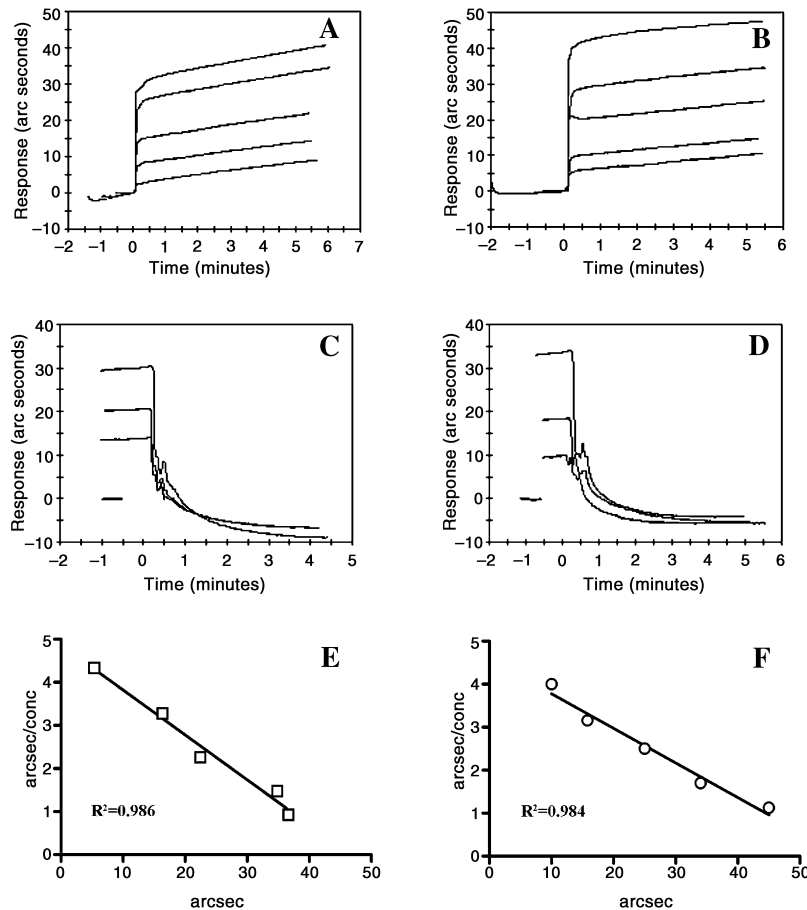


**Fig. 4. TCR V $\beta$ 5.2-SSA interaction analysis.** Association curves between V $\beta$ 5.2 (2.5, 5, 10, 20 and 40  $\mu$ M) and immobilized SSA (A) or SSA(C26S) (B). Data sets were measured five minutes after injection. Dissociation curves between V $\beta$ 5.2 (10, 20, 40  $\mu$ M) and SSA (C) and SSA(C26S). (D). Scatchard analysis for the binding of V $\beta$ 5.2-SSA with a  $K_d = 10.04 \mu$ M (E) and V $\beta$ 5.2-SSA(C26S) with a  $K_d = 10.72 \mu$ M (F).

**Table 1. Binding parameters for SA $\alpha$ -TCR interactions.** Dissociation rate constants ( $k_{diss}$ ) were obtained with FASTPLOT;  $K_d$  were obtained by Scatchard analysis and association rate constants were calculated as  $K_{ass} = K_{diss}/K_d$ . -, No binding detected.

SA $\alpha$ -TCR	$K_{ass}$ ( $M^{-1}\cdot s^{-1}$ ) $\times 10^2$	$K_{diss}$ ( $s^{-1}$ ) $\times 10^{-3}$	$K_d$ (M) $\times 10^{-6}$
wtSSA-V $\beta$ 5.2	34.4	$34.5 \pm 0.6$	10.0
wtSSA-V $\beta$ 2.1	-	-	-
wtSSA-V $\beta$ 1	5.1	$5.5 \pm 0.2$	10.8
SSA(C26S)-V $\beta$ 5.2	29.9	$32.0 \pm 0.5$	10.7
SSA(C26S)-V $\beta$ 2.1	-	-	-
SSA(C26S)-V $\beta$ 1	5.6	$5.1 \pm 0.1$	9.1

no Cys in the mature protein sequence (TSST-1, SPEB, SMEZ1 and 2), three have one Cys (SEI, SEK and SPEC), two have three Cys (SEG and SPEA) and only SSA has more than that, five Cys. As discussed later, the fact that SSA has two Cys residues (Cys26 and Cys101) exposed to solvent would facilitate formation of an intermolecular disulfide bond, as observed in recombinant wtSSA.

In order to address whether dimerization is an artefact of overexpression in *E. coli* we analyzed the supernatant of several *S. pyogenes* isolates by immunoblotting using a rabbit SSA antiserum. As shown in Fig. 6 there is high degree of naturally occurring dimerization in eight out of

ten supernatants studied, which reverted upon DTT treatment of the samples. Further studies are necessary to understand the biological significance of the natural dimerization.

The presence of a dimer in wtSSA, which could not be completely separated from the monomer, prompted us to follow two strategies to obtain a single species; reduction and alkylation, and mutation of the Cys implicated in the intermolecular disulfide bridge. Analysis of the three-dimensional structure of SSA [31] to determine which of the remaining three Cys residues could be implicated in the intermolecular disulfide bridge, showed that Cys158 is located in the core of the protein and is therefore not exposed to solvent. Cys101 could not be identified in the SSA structure because it forms part of the flexible disulfide loop of positions 93-110 with high intrinsic mobility [31]. Cys26 is exposed to solvent in the cleft between the small and large domains, which has been shown to be the TCR binding site in other SA $\alpha$ s. Point mutation of Cys26 to Ser prevented dimer formation and allowed TCR interaction studies.

Initial binding experiments using a biosensor gave an apparent dissociation constant for the immobilized TCR V $\beta$ 5.2 of wtSSA of 153  $\mu$ M, which is near the lower limits of the known SA $\alpha$ -TCR interactions [26]. To avoid any altered  $K_d$  determination due to the immobilization process of the TCR, we immobilized wtSSA to analyze binding to soluble V $\beta$ 5.2 obtaining an approximately 10 times lower  $K_d$ . The  $K_d$  calculation is independent of the amount of

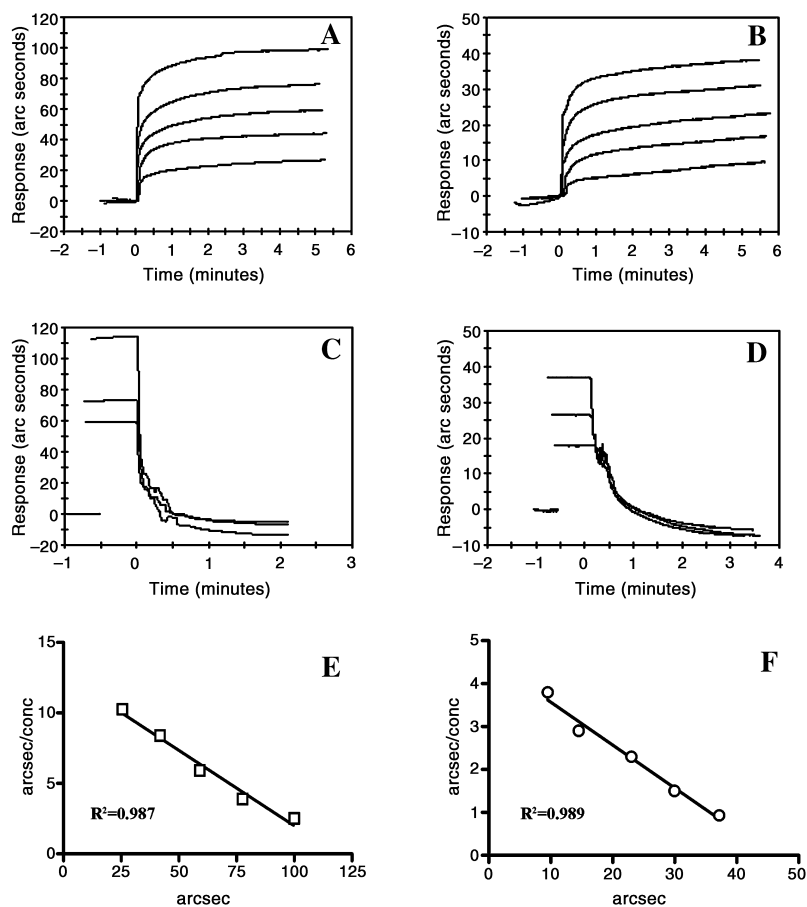


**Fig. 5.** Vβ1-SSA interaction analysis. Association curves between Vβ1 (2.5, 5, 10, 20 and 40 μM) and immobilized SSA (A) or SSA(C26S) (B). Data sets were measured five minutes after injection. Dissociation curves between Vβ1 (10, 20, 40 μM) and SSA (C) or SSA(C26S) (D). Scatchard analysis for the binding of Vβ1-SSA with  $K_d = 10.82 \mu\text{M}$  (E) and Vβ1-SSA(C26S) with a  $K_d = 9.14 \mu\text{M}$  (F).

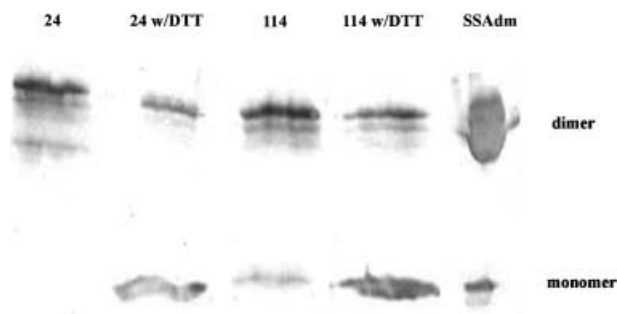


**Fig. 6.** SSA dimer in supernatant of *S. pyogenes*. Supernatants of isolates from patients infected with *S. pyogenes* were analyzed by SDS/PAGE and immunoblotting using a rabbit anti-SSA serum. Lanes 1 and 3: supernatants of 2 isolates; Lanes 2 and 4: supernatants treated with DTT prior SDS/PAGE showing an increase of the monomer; Lane 5: recombinant SSA produced in *E. coli*.

immobilized ligand [29]; consequently, the 5–10% of biologically active monomer contained in the wtSSA allowed an accurate affinity determination when immobilized but gave a 10–20 times higher  $K_d$  when passed over Vβ5.2, as observed. To verify Vβ5.2 availability when immobilized, soluble SSAm and SSA(C26S) were assayed yielding a  $K_d$  similar to wtSSA (150 μM). This demonstrates that the immobilization process affects the binding ability of

the Vβ5.2 in a similar manner as reported for TCR β chain, Vβ8.2 [26]. On the contrary, immobilization of monomer wtSSA and SSA(C26S) yielded a  $K_d = 10 \mu\text{M}$  with soluble Vβ5.2, thus confirming the dissociation constant value for the couple SAg-TCR. In addition, these experiments showed that the C26S mutation was nondisruptive for binding to Vβ5.2.

The superantigen activity of SSA and the likelihood that dimerization occluded its TCR binding site were confirmed in human T-cell stimulation assays where SSAm and SSA(C26S) produced a higher proliferation than the positive control SEC3, which was two orders of magnitude greater than by SSAd. The residual biological activity of this sample could be explained by the SSAm contaminant (Fig. 1B).

Previous studies have shown differences in the Vβ repertoire of native and recombinant SSA. Thus, proliferation assays carried out by Reda *et al.* [21] showed that native SSA-1 but not the recombinant form, was able to stimulate T-lymphocytes bearing Vβ5.2 and Vβ1 TCRs. Similarly, native SSA-2 but not recombinant SSA-2 stimulated T-cells bearing Vβ2 [21]. Differences in the stimulation properties between SSA-1 and SSA-2 cannot be attributed to amino acid sequences because they only differ at residue 2 (Ser and Arg, respectively), which is not expected to be implicated in TCR binding. Here we found that both recombinant wtSSA and SSA(C26S) were able to bind these β chains with detectable affinity using biosensor technology.

**Table 2. Residues of SEB and SEC3 that are implicated in the V $\beta$ 8.2 interaction.** Numbering corresponds to SSA residues. Identical residues are shown as dashes.

SAg	19	20	23	26	60	90	91	173	207
SEB	G	L	N	V	N	Y	Y	F	Q
SEC3	–	T	–	Y	–	–	V	–	–
SSA	–	V	–	C	–	–	–	–	–
SPEA	K	N	–	F	–	–	H	N	–

On the contrary, we did not detect any significant binding between these SAg and V $\beta$ 2.1, which is in accordance with previous cellular proliferation assays [19–21]. A nonproper folding of V $\beta$ 2.1 can be ruled out because it binds toxic shock syndrome toxin-1 [35] and its three-dimensional structure was determined as a complex with the SAg SPEC [36]. The possibility that V $\beta$  specificity may be determined not only by SAg sequence variation within conserved regions, but also by the orientation that a SAg adopts after binding to a class II molecule, or by a particular subset of the presenting class II molecules, cannot be discarded [22]. On the other hand, it has been proposed that a small increase in the affinity of a SAg for MHC can overcome a large decrease in the SAg's affinity for the TCR [30,37].

The kinetic interaction studies of SSA with V $\beta$ 1 and V $\beta$ 5.2 showed a very fast dissociation rate, as observed in TCR–peptide–MHC interactions. In the latter case a single peptide–MHC complex is thought to sequentially bind and trigger a large number of TCRs (up to 200), as proposed in the so-called ‘serial engagement’ model of Lanzavecchia *et al.* [38]. A similar mechanism could be employed by the SAg, which are able to cause TSS in human when 1–2  $\mu$ g is injected [39].

SSA shares with the staphylococcal superantigens, SEB and SEC3, specificity for several mouse and human TCRs, including mouse V $\beta$ 8.2 (M. C. De Marzi & E. L. Malchiodi, unpublished results). The three-dimensional structures of SEB and SEC3 bound to mouse V $\beta$ 8.2 have already been determined [12,13], allowing identification of the most important residues in the TCR binding site. Residues N23, Y90 and Q207, which make the greatest energetic contribution ( $> 2.5$  kcal·mol $^{-1}$ ) [29] to stabilizing the V $\beta$ 8.2–SEC3 complex, are strictly conserved in SEB, SSA and SPEA (Table 2), providing a basis for understanding why these SAg have similar specificity for this TCR  $\beta$  chain. Moreover, residues N23, N60 and Y90 are conserved among bacterial SAg reactive with mouse V $\beta$ 8.2, including SEC1–3, SPEA and SSA. The differences in residues C26 and Y91 in SSA compared with Y26 and V91 in SEC3, which make a slightly lower energetic contribution (1.5–2.0 kcal·mol $^{-1}$ ), can account for the different specificities among SSA (human 1, 2, 19; mouse 14), SEB and SEC3. As shown in Table 2, SSA residues most likely to bind V $\beta$  chains are more similar to those presented in the staphylococcal SEC3 and SEB than in the streptococcal SPEA, indicating that SSA behaves more like a staphylococcal than a streptococcal SAg. The presence of a Cys at position 26 in SSA instead of Tyr, as in SEB, could explain why dimerization mediated by this residue occludes the TCR interaction site.

SAg mutated in the TCR or MHC II binding site could be used to generate protective responses without systemic effects such as TSS and food poisoning. Such recombinant proteins could also be used against tumors or to treat autoimmune diseases [40]. Consequently, the molecular studies of the interaction of SAg with their specific ligands will not only advance understanding of the physiological mechanisms of these molecules, but may lead to the development of therapeutic agents.

## Acknowledgements

This research was supported by Universidad de Buenos Aires; Consejo Nacional de Investigaciones Científicas y Técnicas (CONICET), Agencia Nacional de Investigaciones Científicas y Técnicas (PICT 3440) and Fundación Antorchas, Argentina (E.L.M.). E.J.S. (AI 55882) and R.A.M. are supported by grants from the National Institutes of Health.

## References

- Marrack, P. & Kappler, J. (1990) The staphylococcal enterotoxins and their relatives. *Science* **248**, 705–711.
- Fraser, J., Arcus, V., Kong, P., Baker, E. & Proft, T. (2000) Superantigens - powerful modifiers of the immune system. *Mol. Med. Today* **6**, 125–132.
- Yarwood, J.M., Leung, D.Y. & Schlievert, P.M. (2000) Evidence for the involvement of bacterial superantigens in psoriasis, atopic dermatitis, and Kawasaki syndrome. *FEMS Microbiol. Lett.* **192**, 1–7.
- Leung, D.Y.M., Huber, B.T. & Schlievert, P.M. (1997) Superantigens. In *Molecular Biology, Immunology and Relevance to Human Disease*. Marcel Dekker, Inc, New York, NY.
- McCormick, J.K., Yarwood, J.M. & Schlievert, P.M. (2001) Toxic shock syndrome and bacterial superantigens: an update. *Annu. Rev. Microbiol.* **55**, 77–104.
- Sundberg, E.J., Li, Y. & Mariuzza, R.A. (2002) So many ways of getting in the way: diversity in the molecular architecture of superantigen-dependent T-cell signaling complexes. *Curr. Opin. Immunol.* **14**, 36–44.
- Zhao, Y., Li, Z., Drozd, S.J., Guo, Y., Mourad, W. & Li, H. (2004) Crystal structure of *Mycoplasma arthritis* mitogen complexed with HLA-DR1 reveals a novel superantigen fold and a dimerized superantigen-MHC complex. *Structure* **12**, 277–288.
- Donadini, R., Liew, C.W., Kwan, A.H., Mackay, J.P. & Fields, B.A. (2004) Crystal and solution structures of a superantigen from *Yersinia pseudotuberculosis* reveal a jelly-roll fold. *Structure* **12**, 145–156.
- Hamad, A.R., Marrack, P. & Kappler, J.W. (1997) Transcytosis of staphylococcal superantigen toxins. *J. Exp. Med.* **185**, 1447–1454.
- Papageorgiou, A.C. & Acharya, K.R. (2000) Microbial superantigens: from structure to function. *Trends Microbiol.* **8**, 369–375.
- Hakansson, M., Petersson, K., Nilsson, H., Forsberg, G., Bjork, P., Antonsson, P. & Svensson, L.A. (2000) The crystal structure of staphylococcal enterotoxin H: implications for binding properties to MHC class II and TCR molecules. *J. Mol. Biol.* **302**, 527–537.
- Fields, B.A., Malchiodi, E.L., Li, H., Isern, X., Stauffacher, C.V., Schlievert, P.M., Karjalainen, K. & Mariuzza, R.A. (1996) Crystal structure of a T cell receptor  $\beta$  chain complexed with a superantigen. *Nature* **384**, 188–192.
- Li, H., Llera, A., Tsuchiya, D., Leder, L., Ysern, X., Schlievert, P.M., Karjalainen, K. & Mariuzza, R.A. (1998) Three-dimensional structure of the complex between a T cell receptor  $\beta$  chain and the superantigen Staphylococcal enterotoxin B. *Immunity* **9**, 807–816.



14. Lavoie, P.M., Thibodeau, J., Erard, F. & Sekaly, R.P. (1999) Understanding the mechanism of action of bacterial superantigens from a decade of research. *Immunol. Rev.* **168**, 257–269.
15. Li, Y., Li, H., Dimasi, N., McCormick, J.K., Martin, R., Schuck, P., Schlievert, P.M. & Mariuzza, R.A. (2001) Crystal structure of a superantigen bound to the high-affinity, zinc-dependent site on MHC class II. *Immunity* **14**, 93–104.
16. Li, H., Llera, A., Malchiodi, E.L. & Mariuzza, R.A. (1999) The structural basis of T cell activation by superantigens. *Annu. Rev. Immunol.* **17**, 435–466.
17. McCormick, J.K., Tripp, T.J., Olmsted, S.B., Matsuka, Y.V., Gahr, P.J., Ohlendorf, D.H. & Schlievert, P.M. (2000) Development of streptococcal pyrogenic exotoxin C vaccine toxoids that are protective in the rabbit model of toxic shock syndrome. *J. Immunol.* **165**, 2306–2312.
18. Mollick, J.A., Miller, G.G., Musser, J.M., Cook, R.G., Grossman, D. & Rich, R.R. (1993) A novel superantigen isolated from pathogenic strains of *Streptococcus pyogenes* with aminoterminal homology to staphylococcal enterotoxins B and C. *J. Clin. Invest.* **92**, 710–719.
19. Reda, K.B., Kapur, V., Mollick, J.A., Lamphear, J.G., Musser, J.M. & Rich, R.R. (1996) Molecular characterization and phylogenetic distribution of the Streptococcal superantigen gene (ssa) from *Streptococcus pyogenes*. *Infect. Immun.* **62**, 1867–1874.
20. Stevens, K.R., Van, M., Lamphear, J.G. & Rich, R.R. (1996) Altered orientation of streptococcal superantigen (SSA) on HLA-DR1 allows unconventional regions to contribute to SSA V $\beta$  specificity. *J. Immunol.* **157**, 4970–4978.
21. Stevens, K.R., Van, M., Lamphear, J.G., Orkiszewski, R.S., Ballard, K.D., Cook, R.G. & Rich, R.R. (1996) Species-dependent post-translational modification and position 2 allelism. *J. Immunol.* **157**, 2479–2487.
22. Martin, R., Howell, M.D., Jaraquemada, D., Flerlage, M., Richert, J., Brostoff, S., Long, E.O., McFarlin, D.E. & McFarland, H.F. (1991) A myelin basic protein peptide is recognized by cytotoxic T cells in the context of four HLA-DR types associated with multiple sclerosis. *J. Exp. Med.* **173**, 19–24.
23. Martin, R., Utz, U., Coligan, J.E., Richert, J.R., Flerlage, M., Robinson, E., Stone, R., Biddison, W.E., McFarlin, D.E. & McFarland, H.F. (1992) Diversity in fine specificity and T cell receptor usage of the human CD4<sup>+</sup> cytotoxic T cell response specific for the immunodominant myelin basic protein peptide 87–106. *J. Immunol.* **148**, 1359–1366.
24. Kubo, R.T., Born, J.W., Kappler, J., Marrack, P. & Pigeon, M. (1989) Characterization of a monoclonal antibody which detects all murine  $\alpha\beta$  T cell receptor. *J. Immunol.* **142**, 2736–2742.
25. Bentley, G.A., Boulot, G., Karjalainen, K. & Mariuzza, R.A. (1995) Crystal structure of the beta chain of a T-cell antigen receptor. *Science* **267**, 1984–1987.
26. Malchiodi, E.L., Eisenstein, E., Fields, B.A., Ohlendorf, D.H., Schlievert, P.M., Karjalainen, K. & Mariuzza, R.A. (1995) Superantigen binding to a T cell receptor  $\beta$  chain of known three-dimensional structure. *J. Exp. Med.* **182**, 1833–1845.
27. Ward, E.S. (1992) Secretion of T-cell receptor fragments from recombinant *Escherichia coli* cells. *J. Mol. Biol.* **224**, 885–890.
28. Karlsson, R., Michaelsson, A. & Mattson, L. (1991) Kinetic analysis of monoclonal antigen–antibody interactions with a new biosensor based analytical system. *J. Immunol. Methods* **145**, 229–240.
29. Johnsson, B., Lofas, S. & Lindquist, G. (1991) Immobilization of proteins to a carboxymethylated dextran modified gold surface for biospecific interaction analysis in surface plasmon resonance. *Anal. Biochem.* **198**, 268–277.
30. Leder, L., Llera, A., Lavoie, P.M., Lebedeva, M.I., Li, H., Sekaly, R.P., Bohach, G.A., Gahr, P.J., Schlievert, P.M., Karjalainen, K. & Mariuzza, R.A. (1998) A mutational analysis of the binding of staphylococcal enterotoxins B and C3 to the T cell receptor  $\beta$  chain and major histocompatibility complex class II. *J. Exp. Med.* **187**, 823–833.
31. Sundberg, E.J. & Jardetzky, T.S. (1999) Structural basis for HLA-DQ binding by the streptococcal superantigen SSA. *Nat. Struct. Biol.* **6**, 123–129.
32. Sundstrom, M., Abrahmsen, L., Antonsson, P., Mehindate, K., Mourad, W. & Dohlsten, M. (1996) The crystal structure of staphylococcal enterotoxin type D reveals Zn<sup>2+</sup>-mediated homodimerization. *EMBO J.* **15**, 6832–6840.
33. Roussel, A., Anderson, B.F., Baker, H., Fraser, J.D. & Baker, E.N. (1997) Crystal structure of the streptococcal superantigen SPE-C: dimerization and zinc binding suggest a novel mode of interaction with MHC class II molecules. *Nat. Struct. Biol.* **4**, 635–643.
34. Papageorgiou, A.C., Gutman, D.M., Kline, J.B., O'Brien, S.M., Tranter, H.S. & Acharya, K.R. (1999) Structural basis for the recognition of superantigen streptococcal pyrogenic exotoxin A (SpeA1) by MHC class II molecules and T-cell receptors. *EMBO J.* **18**, 9–21.
35. McCormick, J.K., Tripp, T.J., Llera, A.S., Sundberg, E.J., Dinges, M.M., Mariuzza, R.A. & Schlievert, P.M. (2003) Functional analysis of the TCR binding domain of toxic shock syndrome toxin-1 predicts further diversity in MHC class II/superantigen/TCR ternary complexes. *J. Immunol.* **171**, 1385–1392.
36. Sundberg, E.J., Li, H., Llera, A.S., McCormick, J.K., Tormo, J., Schlievert, P.M., Karjalainen, K. & Mariuzza, R.A. (2002) Structures of two streptococcal superantigens bound to TCR  $\beta$  chains reveals diversity in the architecture of T cell signaling complexes. *Structure* **10**, 687–699.
37. Li, H., Llera, A. & Mariuzza, R.A. (1998) Structure–function studies of T-cell receptor–superantigen interactions. *Immunol. Rev.* **163**, 177–186.
38. Valitutti, S., Muller, S., Cella, M., Padovan, E. & Lanzavecchia, A. (1995) Serial triggering of many T-cell receptors by a few peptide-MHC complexes. *Nature* **375**, 148–151.
39. Dinges, M.M., Orwin, P.M. & Schlievert, P.M. (2000) Exotoxins of *Staphylococcus aureus*. *Clin. Microbiol. Rev.* **13**, 16–34.
40. Hong-Geller, E. & Gupta, G. (2003) Therapeutic approaches to superantigen-based diseases: a review. *J. Mol. Recognit.* **16**, 91–101.